Design, Synthesis and Photophysical Analysis of New Unsymmetrical Carbazole-Based Dyes for Dye-Sensitized Solar Cells

Faegheh Ghasempour Nesheli, Mahmood Tajbakhsh, Behzad Hosseinzadeh, Rahman Hosseinzadeh

PII: S1010-6030(20)30320-8

DOI: https://doi.org/10.1016/j.jphotochem.2020.112521

Reference: JPC 112521

To appear in: *Journal of Photochemistry & Photobiology, A: Chemistry*

Received Date: 19 January 2020

Revised Date: 12 March 2020

Accepted Date: 26 March 2020

Please cite this article as: Nesheli FG, Tajbakhsh M, Hosseinzadeh B, Hosseinzadeh R, Design, Synthesis and Photophysical Analysis of New Unsymmetrical Carbazole-Based Dyes for Dye-Sensitized Solar Cells, *Journal of Photochemistry and amp; Photobiology, A: Chemistry* (2020), doi: https://doi.org/10.1016/j.jphotochem.2020.112521

Design, Synthesis and Photophysical Analysis of New Unsymmetrical Carbazole-Based Dyes for Dye-Sensitized Solar Cells

Faegheh Ghasempour Nesheli [a], Mahmood Tajbakhsh [a,*], Behzad Hosseinzadeh [a], Rahman Hosseinzadeh[a]

[a] *Department of Organic Chemistry, Faculty of Chemistry, University of Mazandaran, Babolsar 47416-95447, Iran*

**Corresponding author E-mail: Tajbaksh@umz.ac.ir*

Graphical abstract

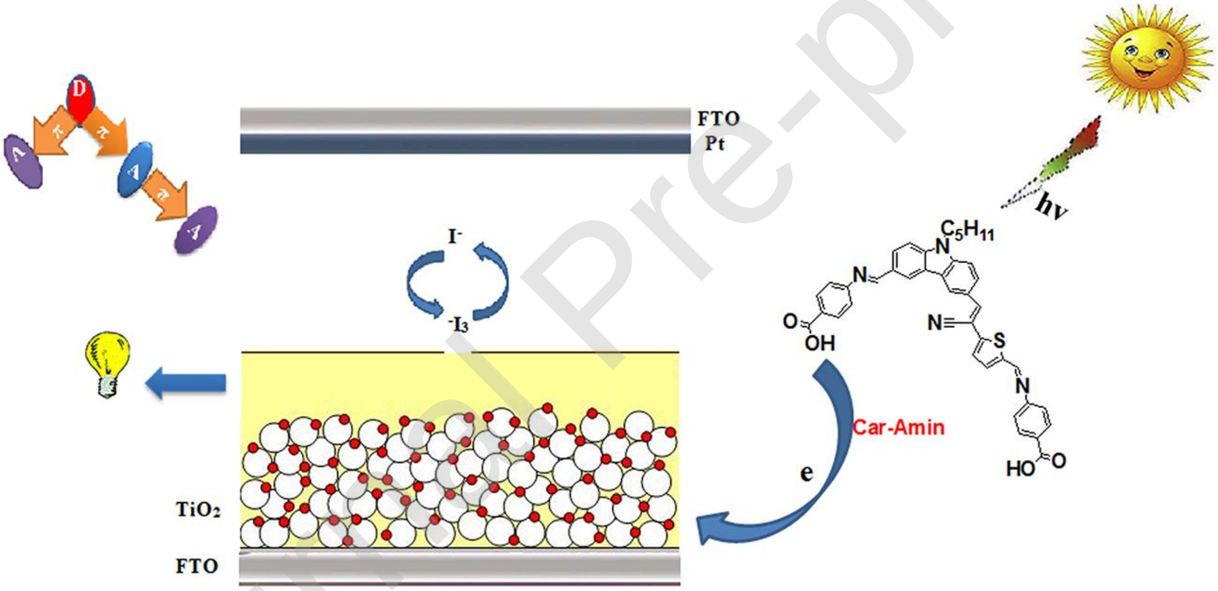

Highlights

- Three new carbazole-based di-anchoring unsymmetrical organic dyes were designed and synthesized for the DSSC application.

- The effect of different acceptor groups on the performance of the prepared DSSCs was studied.
- **Car-Amin** dye with 4-aminobenzoic acid as an acceptor unit exhibited better photovoltaic performance compared to the other dyes.

Abstract

The molecular design, synthesis, and characterization of di-anchoring carbazole-based dyes (Car-Cy, Car-Amin, and Car-Mal) with A-π-D-π-A-π-A structure as materials for dye-sensitized solar cells applications (DSSCs) are reported. The electron-rich carbazole moiety in the structure of synthesized dyes is connected with acceptor/ or anchoring groups (cyanoacetic acid, 4-aminobenzoic acid, and malonic acid) and π-spacers (vinylene and cynovinyl thiophene). Electronic characteristics and molecular geometry of the sensitizers were optimized using Density Functional Theory (DFT), and the influence of dye structure on their photovoltaic performances was studied. Among the synthesized dyes in this research, Car-Amin dye presents a better photovoltaic performance as a sensitizer in the constructed device, with a power conversion efficiency (PCE) of 2.27%, J_{SC} of 5.95 $mAcm^{-2}$, V_{OC} of 0.54 V and FF of 71%. The enhanced performance of this dye could be related to the powerful electron-withdrawing characteristic of the 4-aminobenzoic acid as an acceptor group in the dye structure. Consequently, the impact of various acceptor groups on the constructed DSSC devices was examined, and the results indicated that the

improvement of DSSC performance is due to the presence of 4-aminobenzoic acid as acceptor on the carbazole-based dyes.

Abbreviations

Dye-sensitized solar cells (DSSCs)

Density Functional Theory (DFT)

Cyclic Voltammetry (CV)

Power conversion efficiency (PCE)

Open-circuit photovoltage (V_{oc})

Fill factor (FF)

Short-circuit photocurrent density (J_{SC})

Electrochemical impedance spectroscopy (EIS)

Incident photon-to-current efficiency (IPCE)

Current–voltage (J –V)

Intramolecular charge transfer (ICT)

Highest occupied molecular orbital (HOMO)

Lowest unoccupied molecular orbital (LUMO)

First oxidation potentials (E_{ox})

Frontier molecular orbital (FMO)

Charge recombination resistance (R_{ct})

Electron lifetime (τ)

Chemical capacitances (C_μ)

Dimethylformamide (DMF)

Dimethyl sulfoxide (DMSO)

Phosphorus oxychloride ($POCl_3$)

Ethanol (EtOH)

Methanol (MeOH)

Acetic acid (AcOH)

Ammonium acetate (NH_4OAc)

Keywords: Dye-sensitized solar cell (DSSC), Carbazole, 4-aminobenzoic acid, Cyanoacetic acid, Malonic acid.

Introduction

The necessity of using non-expensive renewable energy has attracted many researchers to focus on organic photovoltaic material. Many researchers have concentrated on the DSSCs based on mesoporous TiO_2 thin films because of their low-cost and suitable PCE [1]. Photosensitizers as the most vital and major components of DSSCs have a considerable task in the light harvesting process for electricity generation. The Ruthenium complexes like N3, N719, and NCSU-10 are excellent light harvesting compounds in DSSCs because of their good optical and electrochemical behavior [2]. Although the maximum PCE for such DSSCs is reported to be more than 10%, some disadvantages including the utilization of expensive noble metals, unavailability, high cost of preparation, being detrimental to the environment and having problematic separation have limited their further applications [3-9]. Moreover, the sensitizers without metal in their structures have become more popular compared to Ruthenium complexes because of their design versatility, easy availability, convenient synthesis, low cost, high capability of light harvesting, easy purification and being environment-friendly [10-13]. Organic sensitizers usually employ donor–π–acceptor (D–π–A) architecture, which includes a donor (D) that is connected to an acceptor unit (A) via a π-linker (π). Recently, series of indolo[3,2,1-jk]carbazole- based organic dyes with the D-π-A architecture synthesized and the effect of different π-bridges on photovoltaic performance have been studied [14, 15].

The donor groups of the dyes are important components in DSSCs because of their effects on the absorption properties and energy levels [16, 17]. Typically, various compounds including coumarin [18], squaraine [19], indoline [20], phenothiazine (PTZ) [21], triphenylamine [22], fluorene [20], carbazole [23] and tetrahydroquinoline [24] have been used as electron-donating moieties in most of the organic dyes. Among the mentioned donors, as can be observed in Figure 1, carbazole is an aromatic tricyclic compound, containing pyrrole and benzene rings. The donor and hole-transporting properties of carbazole are mostly due to the existence of the pyrrole ring in its structure. Up to 240°C, the carbazole system is thermally stable, and this stability can be improved even more by attaching it to other molecules. Carbazole is cheap, easily available, and if necessary its solubility in organic solvents can be improved by functionalizing its nitrogen atom with alkyl groups [25]. The organic dyes on the basis of carbazole were first developed in 2006. After that, many carbazole-based dyes were prepared and employed in DSSCs as donor or π-spacer [26, 27]. Further, many carbazole-based hole-transporting materials (HTMs) were synthesized and employed in perovskite solar cells as donor or π-spacer [28, 29].

For improving the performance of DSSCs, the π-conjugated units have a critical task in the architecture of metal-free organic dyes. It is known that thiophene derivatives are employed as π-conjugated groups because of their unique electrochemical and polarizability properties as well as their good charge transporting ability [13]. However, the synthetic procedure of connecting thiophene derivatives to the carbazole ring system is usually complicated and needs costly metal catalysts under anhydrous and inert conditions [30, 31]. To overcome these problems, Knoevenagel condensation reaction of thiophene-2-acetonitrile with aldehydes can be easily used to introduce the thiophene derivatives onto the carbazole ring system. The advantage of this synthetic route is the introduction of thiophene moiety and cyanovinyl group to the carbazole ring system, which leads to the extension of π-conjugations as well as the reduction of the gap between LUMO and HOMO energy levels.

Recently, the advantages of using 4-aminobenzoic acid, cyanoacetic acid, and malonic acid as effective electron acceptors for fabricating DSSCs including their powerful electron-withdrawing properties as well as having the capability of connecting onto the TiO_2 surface via carboxylic acid have drawn much attention from the researchers [32]. Furthermore, di-anchoring organic sensitizers reported in the literature exhibit several advantages including multi binding abilities to TiO_2 nanoparticles, the red shift in UV-absorption, and a more desirable electron injection which improves the generated photocurrent [33-37]. Studies have indicated that employing di-anchoring organic dyes instead of single D–π–A dyes in DSSCs results in a better PCE [9, 38-42].

Di-anchoring sensitizers provide lower open-circuit photovoltage (V_{oc}) in comparison with similar mono-anchoring sensitizers. This is assumed to be related to the undesirable improved charge recombination process in these sensitizers [37]. Thus, the structure of di-anchoring sensitizers can be optimized to achieve DSSCs with higher efficiencies. There are many symmetrical di-anchoring sensitizers that have been reported in the literature, however, there are not many reports on the asymmetric di-anchoring sensitizers.

In this regard, this research has aimed to design three novel A- π -D-π-A- π-A configurated dyes (Car-Cy, Car-Amin, Car-Mal) containing two acceptor/or anchoring units and one donor group (Figure 1). The new asymmetrical di-anchoring sensitizers have a carbazole moiety, which plays the role of the donor, and a π-conjugated fragment (cyano vinylene and thiophene groups) that is attached to acceptor group on one side, whereas an acceptor unit is connected to carbazole on the other side. Cyanoacetic acid, 4-aminobenzoic acid, and malonic acid in the structure of the synthesized dyes act as electron acceptor/anchoring units.

Figure 1 shows the structure of the synthesized dyes. These dyes were analyzed using various spectral methods such as ^{1}H and ^{13}C NMR, mass spectroscopy, CHN examination, and FT-IR. The electrochemical and optical behavior of these synthesized dyes were also examined to evaluate the effects of the anchoring groups in their structure. The constructed devices using the synthesized dyes were investigated for photovoltaic performance and electrochemical impedance spectroscopy (EIS) behavior.

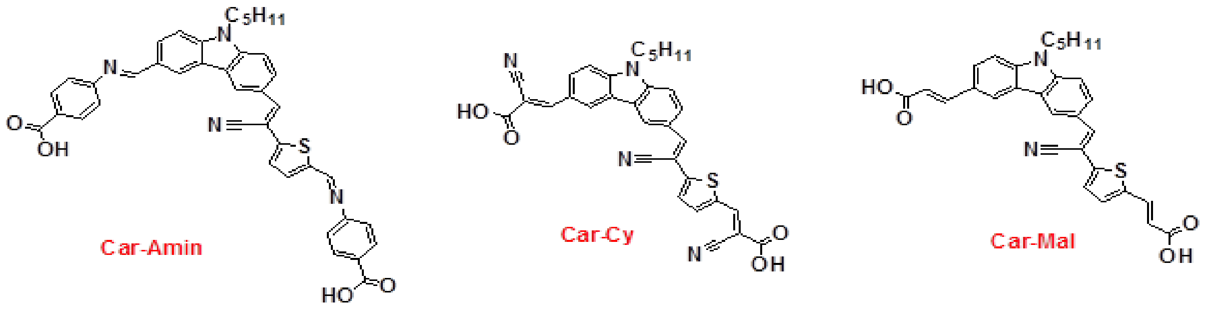

Figure. 1 The chemical structures of Car-Cy, Car-Amin and Car-Mal dyes.

2 The Experimental

2.1 Equipment and materials

The chemicals and solvents were bought from Aldrich and Merck companies. These materials were utilized without further purification. The samples were examined using an FT-IR Bruker Vector 22 spectrometer. A Bruker 400 MHz Ultrashield Avance DRX spectrometer was used for analyzing ^{1}H and ^{13}C NMR spectra, using DMSO-d$_6$ and CDCl$_3$ as solvents. Electrothermal 9100 apparatus (UK) was used to measure melting points of samples. A Finnigan-Matt 8430 mass spectrometer was employed for recording the mass spectra at the ionization potential of 70 eV. A LECO-600 CHN Elemental Analyzer was used in order to perform elemental analysis.

The UV/VIS absorption spectra were examined using Jasco V-750 spectrophotometer. Further, the fluorescence emission spectra were recorded using Jasco FP-8300 fluorescence spectrophotometer. Cyclic Voltammetry (CV) experiments were conducted by VersaSTAT 4 Potentiostat Galvanostat (Princeton Applied Research), connected to a regular 3-electrode system which included a glassy carbon working electrode, a platinum counter electrode, and an Ag/AgCl reference electrode in a DMF solution with room temperature. The potentials were recorded with a scan rate of 0.05 Vs^{-1}, and the solution of the samples was prepared using the 10^{-4} M sample and also 0.1 M tetrabutylammonium tetrafluoroborate as the supporting electrolyte. An AM 1.5G solar simulator (Sharif Solar, SIM-1000, light intensity: 100 mW/cm^2) was used for photovoltaic evaluation of the prepared cells. A Bio-Logic SAS SP-300 was utilized for measuring the current–voltage (J –V). Also, an IPCE system with a 100 W halogen lamp (Sharif Solar, IPCE-015) was employed to determine the incident photon-to-current efficiency (IPCE). The electrochemical impedance spectroscopy (EIS) were measured on an impedance analyzer (EIS-25H, Sharif Solar) at their open-circuit photovoltage (V_{oc}).

2.2. The synthetic process and characterization

The synthesis of the novel carbazole-based dyes was performed as it has been shown in scheme 1. The synthesizing process involved a series of synthetic procedures such as N-alkylation, Vilsmeier-Haack, and Knoevenagel condensation reaction. The synthesizing procedure of the intermediates and dyes, as well as their spectral data, have been reported in the following sections.

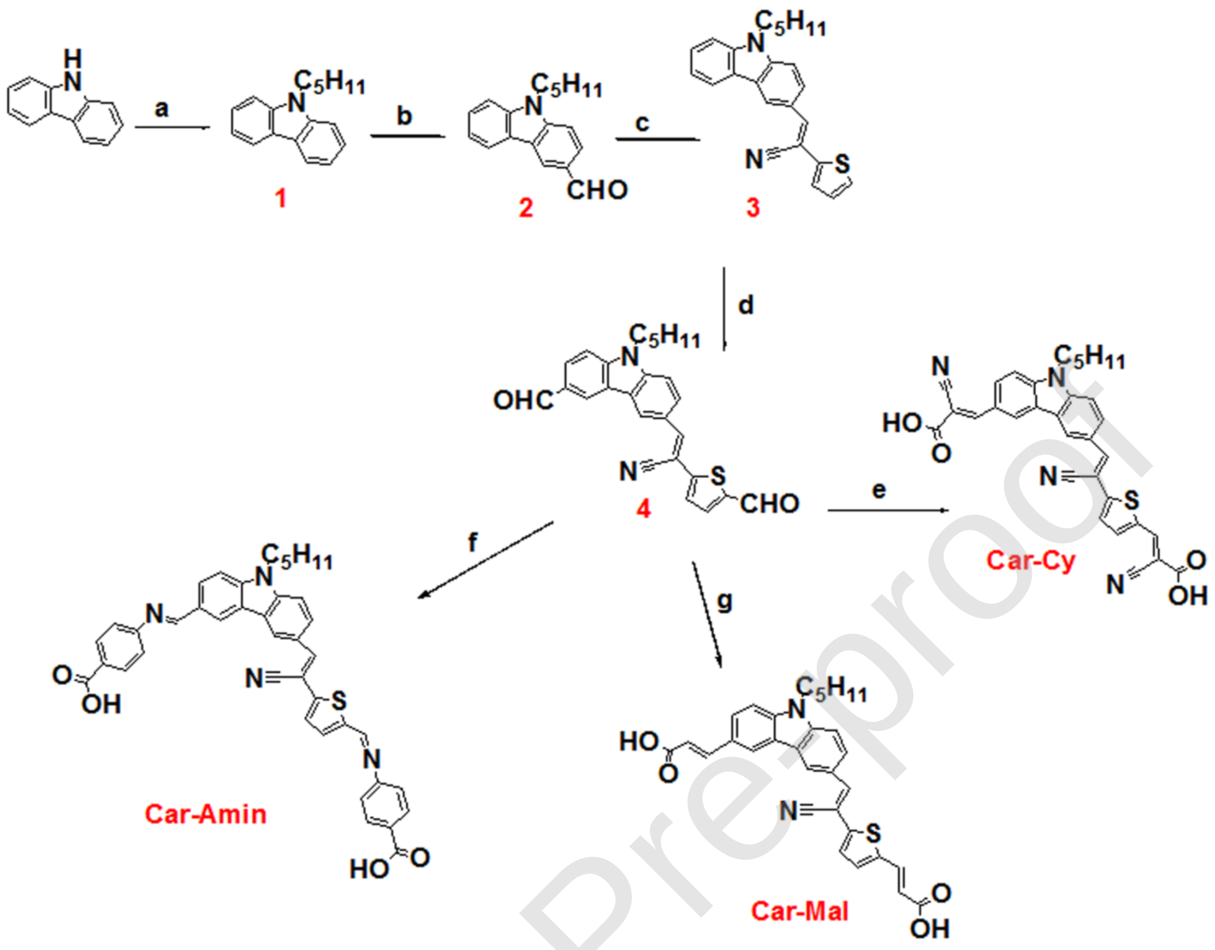

Scheme 1. The pathway of synthesizing for the novel carbazole-based dyes. **a** 1-bromopentane, NaOH, DMSO, 110 °C; **b** $POCl_3$, DMF, 100 °C; **c** thiophene-2-acetonitrile, EtOH, reflux; **d** $POCl_3$, DMF, 100 °C; **e** cyanoacetic acid, AcOH, NH_4OAc, reflux; **f** 4-aminobenzoic acid, MeOH, reflux; **g** malonic acid, piperidine, pyridine, reflux.

2.2.1 The procedure of synthesizing 9- pentyl-9H-carbazole (1)

In order to synthesize compound 1, a previously reported technique was utilized with some adjustments [43]. A mixture of carbazole (2.0 g, 0.01196 mol), 1-bromopentane (3.071 g, 0.02033 mol), dimethylsulfoxide (DMSO) (30 mL), and sodium hydroxide (4.0 g, 0.10046 mol) underwent stirring at 110 °C for 12 hours. Subsequently, the mixture temperature was reduced to 25 °C by leaving it in the room. Then, hexane and water were employed for extracting the product. A rotary evaporator was utilized in order to evaporate the organic solvent under a vacuum condition. The remaining solid material underwent a purification process by silica gel column chromatography with hexane as an eluent, and consequently a white solid was generated (92%, 2.61 g). m.p; 51-52 °C, ^{1}H NMR (300 MHz, $CDCl_3$): δ 8.18 (d, 2H, J = 8 Hz), 7.55–7.51 (m, 2H), 7.47–7.45 (m, 2H), 7.29 (t, 2H, J = 7.4 Hz), 4.34 (t, 2H, J = 7.2 Hz), 1.93 (q, 2H, J = 7.2 Hz), 1.44–1.41 (m, 4H), 0.94 (t, 3H, J = 6.8 Hz), ^{13}C NMR (100 MHz, $CDCl_3$): δ 140.47, 125.60, 122.84, 120.38, 118.72, 108.69, 43.08, 29.47, 28.73, 22.55, 14.02.

2.2.2. The procedure of synthesizing 9- pentyl-9H-carbazole-3-carbaldehyde (2)

Initially, a cold DMF solution (1.5 mL, 20 mmol, 0 ^{0}C) was prepared, then phosphorus oxychloride (1.6 mL, 17 mmol) was added to the cold solution dropwise. The mixture underwent stirring for 1 hour at 0 ^{0}C. Afterward, the 9- pentyl-9H-carbazole (1, 3.56 g, 15 mmol) that was produced in the previous section of the study, was added to this mixture, and the mixture was heated at 95 ^{0}C for 7 hours. Subsequently, it was gradually cooled to 25 ^{0}C, and was poured into a mixture of ice and water, also, NaOH (4 M) was employed for basifying the mixture. CH_2Cl_2 and brine were used for extracting the product, and Na_2SO_4 was utilized in order to dry the organic phase. After that, in order to remove the Na_2SO_4, the mixture went through filtration, and the filtrate was evaporated under a vacuum condition. Then, the crude product underwent a purification process using silica gel column chromatography (ethyl acetate/ hexane, 1/10, v/v) to obtain a white powder (70%, 2.78 g), m.p; 63-64 ^{0}C, FT-IR (KBr pellet, cm^{-1}): 2956 (C-H stretching), 1688 (C=O stretching), 1592 (C=C stretching), ^{1}H NMR (300 MHz,$CDCl_3$): δ 10.10 (s, 1H), 8.60 (s, 1 H), 8.16 (d, J=7.6 Hz, 1H) , 8.01 (d, J= 8.4 Hz, 1H), 7.55 (t, J= 8.4 Hz, 1H), 7.47-7.45 (m, 2H), 7.36-7.32 (m, 1H), 4.31

(t, J= 7.2 Hz, 2H) , 1.90 (q, 2H, J = 7.2 Hz), 1.39-1.37 (m, 4H), 0.90 (t, J=7.2 Hz, 3H), ^{13}C NMR (100 MHz, $CDCl_3$): δ 191.79, 144.05, 141.15, 128.45, 127.13, 126.71, 123.98, 123.03, 122.97, 120.73, 120.28, 109.40, 108.93, 43.38, 29.35, 28.64, 22.45, 13.95, Mass: m/z: 265.1, Anal. Calcd. for $C_{18}H_{19}NO$: C, 81.47; H, 7.22; N, 5.28. Found: C, 81.30; H, 7.12; N, 5.32.

2.2.3. The procedure of synthesizing (Z)-3-(9-pentyl-9H-carbazol-3-yl)-2-(thiophen-2-yl) acrylonitrile (3)

A mixture of thiophene-2-acetonitrile (1.44 mL, 13.6 mmol), ethanol (30 mL), compound 2 (3 g, 11.3 mmol), and NaOH (0.1 mL, 6 M) was refluxed for 2 hours. The obtained yellow residue went through filtration, and it was rinsed using methanol. Finally, the recrystallization in chloroform gave a yellow solid as the product with a yield of 72 %, m.p; 104-105 ^{0}C, FT-IR (KBr pellet, cm^{-1}): 2949 (C-H stretching), 2215 (-CN stretching), 1587 (C=C stretching), ^{1}H NMR (400 MHz, $CDCl_3$): δ 8.59 (s, 1H), 8.18-8.10 (m, 2H), 7.58 (s, 1H), 7.53 (t, 1H), 7.47-7.44 (m, 2H), 7.39 (d, 1H, J= 4 Hz), 7.33-7.28 (m, 2H), 7.10 (d, 1H), 4.32 (t, 2H, J= 7.2 Hz), 1.91 (q, 2H, J = 7.2 Hz), 1.41-1.37 (m, 4H) 0.91 (t, 3H, J= 7.2 Hz), ^{13}C NMR (100 MHz, $CDCl_3$): δ 141.61, 141.23, 141.01, 140.17, 128.02, 126.82, 126.44, 125.99, 125.14, 124.39, 123.25, 122.75, 122.45, 120.74, 119.82, 117.95, 109.18, 109.15, 102.05, 43.31, 29.38, 28.70, 22.46, 13.96, Mass: m/z 370.2, Anal. Calcd. for $C_{24}H_{22}N_2S$: C, 77.80; H, 5.98; N, 7.56. Found: C, 77.80; H, 5.92; N, 7.52.

2.2.4. The procedure of synthesizing (Z)-3-(3-formyl-9-pentyl-9H-carbazol-6-yl)-2-(5-formylthiophen-2-yl) acrylonitrile (4)

Phosphorus oxychloride (4.4 ml, 25eq) was added to a cold DMF solution (3.4 ml, 23eq) dropwise under an inert atmosphere at the temperature of 0° C. The mixture underwent stirring for 1 hour. Then, compound 3 (0.74 g, 2 mmol) was added to the mixture, and they underwent stirring again at 100°C for 4 hours. After the reaction was ended (identified by TLC), the mixture temperature was decreased to 25 °C and it was poured into a mixture of water and ice. Afterward this mixture was basified using 4M NaOH. CH_2Cl_2 and brine were used for extracting the product, and Na_2SO_4 was utilized in order to dry the organic phase. Then, a rotary evaporator was used for evaporating the organic solvent under a vacuum condition and the resulting crude product underwent a purification process by the means of silica gel column chromatography (ethyl acetate/ hexane, 1/5, v/v), to obtain an orange colored solid (32%; 0.27 g), m.p; 118 ^{0}C, FT-IR (KBr pellet, cm^{-1}): 2924 (C-H stretching), 2212 (-CN stretching), 1671 (C=O stretching), 1583 (C=C stretching), ^{1}H NMR (400 MHz, $CDCl_3$): δ 10.15 (s, 1H), 9.93 (s, 1H), 8.74 (s, 1H), 8.68 (s, 1H), 8.20-8.09 (m, 2H), 7.78-7.76 (m, 2H), 7.56 (d, 2H, J=8.4 Hz), 7.51 (d, 1H, J=4 Hz), 4.40 (t, 2H, J=7.2 Hz), 1.94 (q, 2H, J = 7.2 Hz), 1.42-1.39 (m, 4H), 0.90 (t, 3H, J=7.2 Hz), ^{13}C NMR (100 MHz, $CDCl_3$) δ 191.54, 182.64, 167.83, 149.07, 144.67, 143.86, 142.51, 137.02, 129.61, 128.47, 127.74, 126.86, 125.08, 123.70, 123.34, 122.89, 119.19, 116.85, 110.14, 109.74, 102.26, 43.87, 31.93, 29.69, 22.39, 14.10, Mass: m/z; 426.2, Anal. Calcd. for $C_{26}H_{22}N_2O_2S$: C, 73.21; H, 5.20; N, 6.57. Found: C, 73.19; H, 5.17; N, 6.50.

2.2.5. The procedure of synthesizing (2*Z*)-3-[5-((*E*)-2-{6-[(*E*)-2-carboxy-2-cyanovinyl]-9-pentyl-9*H*-carbazol-3-yl}-1-cyanovinyl)-2-thienyl]-2-cyanoacrylic acid (Car-Cy)

A mixture of cyanoacetic acid (0.038 g, 0.45 mmol), compound 4 (0.064 g, 0.15 mmol), glacial acetic acid (15 mL) and ammonium acetate (0.057 g, 0.74 mmol) was refluxed for 12 hours. Then the mixture temperature was decreased to 25 °C and it was poured into a mixture of ice and water, to generate a red colored solid. The mixture was then filtered to collect the generated solid. Finally, the crude product underwent a purification process with silica gel column chromatography ($CHCl_3$:CH_3OH, 10:1, v/v) to result in a red colored solid. Yield 58%, m.p; 290 ^{0}C, FT-IR (KBr pellet, cm^{-1}): 3252 (O-H stretching), 2924 (C-H stretching), 2219 (-CN stretching), 1730 (C=O stretching), ^{1}H NMR (400 MHz DMSO-d$_6$,): δ 8.89 (s, 1H), 8.76 (s, 1H), 8.49 (s, 2H), 8.28 (d, 2H, J=9.2 Hz), 8.24 (s, 1H), 8.01 (d, 1H, J=4 Hz), 7.9 (d, 2H, J=8.8 Hz), 7.65 (d, 1H, J=4 Hz), 4.51 (t, 2H, J=7.6 Hz), 1.82 (q, 2H), 1.29-1.23 (m, 4H), 0.82 (t, 3H, J=6.8 Hz), ^{13}C NMR (125 MHz DMSO-d$_6$): δ 164.42, 163.82, 155.23, 148.24, 146.33, 144.90, 143.70, 142.85, 141.10, 139.12, 137.77, 135.62, 129.50, 127.98, 126.65, 125.58, 125.30, 124.37, 123.95, 122.85, 122.80, 117.57, 116.84, 111.48, 100.88, 100.06, 99.97, 43.39, 28.96, 28.71, 22.32, 14.33, Mass: m/z 562. Anal. Calcd. for $C_{32}H_{24}N_4O_4S$: C, 68.56; H, 4.31; N, 9.99. Found C, 68.50; H, 4.29; N, 9.95.

2.2.6. The procedure of synthesizing 4-[((1*E*)-{5-[(*E*)-2-(6-{(*Z*)-[(4-carboxyphenyl)imino] methyl}-9-pentyl-9*H*-carbazol-3-yl)-1-cyanovinyl]-2-thienyl}methylene)amino]benzoic acid (Car-Amin)

A mixture of 4-aminobenzoic acid (0.06 g, 0.45 mmol), dry methanol, and compound 4 (0.064 g, 0.15 mmol) was refluxed for 3 hours. After the filtration and recrystallization of the precipitated product from methanol, a bright orange colored solid was acquired. Yield 77%, m.p; 325 ^{0}C, FT-IR (KBr pellet, cm^{-1}): 3437 (O-H stretching), 2927 (C-H stretching), 2214 (-CN stretching), 1686 (C=O stretching), ^{1}H NMR (400 MHz DMSO-d$_6$): δ 8.88 (s, 1H), 8.82 (d, 2H, J=12 Hz), 8.72 (s, 1H), 8.21-8.17 (m, 2H), 8.15 (s, 1H), 8.01-7.98 (m, 4H), 7.87-7.82 (m, 2H), 7.75 (d, 1H, J=4 Hz), 7.50 (d, 1H, J=4 Hz), 7.38-7.36 (m, 4H), 4.50 (t, 2H, J=6.8 Hz), 1.83 (q, 2H), 1.30-1.28 (m, 4H), 0.82 (t, 3H, J=6.8 Hz), ^{13}C NMR (400 MHz DMSO-d$_6$): δ 167.99, 167.45, 156.23, 155.24, 154.57, 153.59, 144.59, 144.43, 143.49, 143.26, 142.71, 142.54, 142.29, 142.17, 135.62, 131.68, 131.09, 129.46, 128.72, 128.53, 128.26, 127.84, 126.89, 125.59, 122.93, 122.60, 122.51, 121.72, 121.52, 117.62, 117.31, 113.03, 111.22, 101.62, 101.14, 43.22, 28.96, 28.65, 22.30, 14.30 , Mass: m/z 664.2. Anal Calcd. for $C_{40}H_{32}N_4O_4S$: C, 72.27; H, 4.85; N, 8.43. Found: C, 72.20; H, 4.81; N, 8.41.

2.2.7. The procedure of synthesizing (2*E*)-3-[5-((*E*)-2-{6-[(*E*)-2-carboxyvinyl]-9-pentyl-9*H*-carbazol-3-yl}-1-cyanovinyl)-2-thienyl] acrylic acid (Car-Mal)

Initially, a mixture of piperidine (0.05 mL, 0.53 mmol), malonic acid (0.15 g, 1.45 mmol), pyridine (3 mL), and compound 4 (0.20 g, 0.48 mmol), was refluxed for 5 hours. Afterward, the mixture temperature was reduced to 25 ^{0}C, and it was poured into a mixture of water and ice. Then, an HCl solution (2 M) was used in order to acidify the mixture until a red solid is generated. After the filtration and rinsing this solid material with water, a vacuum oven was employed for drying it for 12 hours. Subsequently, in order to purify the precipitate, it was recrystallized from ethanol to result in a dark red colored solid with a yield of 75 %, m.p; 240 ^{0}C, FT-IR (KBr pellet, cm^{-1}): 3428 (O-H stretching), 2929 (C-H stretching), 2213 (-CN stretching), 1683 (C=O stretching), ^{1}H NMR (400 MHz, DMSO-d$_6$): δ 12.38 (s, 2H), 8.74 (s, 1H), 8.51 (s, 1H), 8.19 (d, 1H, J=8.8 Hz), 8.00 (s, 1H), 7.90-7.88 (m, 2H), 7.84-7.82 (m, 1H), 7.78 (d, 1H, J=3.2 Hz), 7.74-7.72 (m, 1H), 7.57 (d, 1H, J=3.6 Hz), 7.45 (d, 1H, J=3.6 Hz), 6.58 (d, 1H, J=16 Hz), 6.22 (d, 1H, J=15.6 Hz), 4.48 (t, 2H), 1.80 (q, 2H), 1.29 (m, 4H), 0.81 (t, 3H, J=6.4 Hz), ^{13}C NMR (100 MHz, DMSO-d$_6$): δ 168.38, 167.56, 145.38, 143.27, 142.39, 142.26, 142.18, 139.32, 138.49, 136.60, 133.37, 132.23, 127.20, 127.01, 126.80, 125.04, 123.79, 122.91, 122.80, 121.73, 118.85, 117.78, 111.02, 104.53, 101.28, 43.50, 29.00, 28.74, 22.34, 14.32, Mass: m/z 509.5. Anal. Calcd. For $C_{30}H_{26}N_2O_4S$: C, 70.57; H, 5.13; N, 5.49. Found: C, 70.51; H, 5.10; N, 5.44.

2.3. The fabrication of titanium dioxide electrode

The titanium dioxide electrode was constructed using the reported method in the literature [44]. A mixture of acetic acid (12 g, 0.2 mol) and titanium isopropoxide (58.6 mg, 0.2 mol) underwent stirring at 25 °C for 15 minutes. Afterward, it was added into water (290 mL) at once and while stirring (600 rpm). The stirring of the mixture was continued for another 1 hour to complete the hydrolysis. Then concentrated nitric acid (4 mL) was added to the mixture, and they underwent stirring at 80 °C for about 40 minutes and were peptized for 75 minutes.The mixture was cooled by adding water to obtain a volume of 370 mL, then it was heated in a titanium autoclave (570 mL) at the temperature of 250 °C for 12 hours.

Subsequently, nitric acid (65%, 2.4 mL) was added to the contents of autoclave at 25 °C and was ultrasonicated with the power of 200 W at the frequency of 20 pulses in every 3 seconds. The obtained solution was evaporated to a concentration of 13 wt% TiO_2. The residue was centrifuged and rinsed using ethanol, to generate a white solid.

2.4. Preparing the DSSC devices

A blocking layer was prepared by treating 40 mM $TiCl_4$ aqueous solution with fluorine-doped tin oxide (FTO) coated glass substrate for half an hour at the temperature of 70 °C. Titania pastes (Sharif Solar Co.) and a doctor blade were used to prepare the photoanodes. The photoanodes were made of transparent and scattering layers of TiO_2 nanoparticles. The scattering layer with a thickness of 5 μm contained TiO_2 nanoparticles in the range of 150–300 nm, while the transparent layer with a thickness of 7 μm contained TiO_2 nanoparticles with a size of 20 nm. Thickness of the TiO_2 layers were measured with a profilometer and confirmed with the cross-sectional scanning electron microscope (SEM) image (Figure S 28).

The FTO films with titanium dioxide coatings were heated for 10 minutes at the temperature of 375 °C, 15 minutes at the temperature of 450 °C, and 30 minutes at the temperature of 500 °C. Then, their temperature was reduced to 25 °C. The obtained films underwent another treatment with a 40 mM $TiCl_4$ aqueous solution at the temperature of 70 °C for half an hour. They were washed using water and heated at a temperature of 500 °C for 30 minutes. Afterward, dye solutions (0.4 mM in DMF) were employed for immersing the titanium dioxide electrodes for 20 hours without the presence of light, and the electrodes were rinsed with water. The FTO glass was coated by the H_2PtCl_6 solution (one drop) to set the counter electrode. This electrode was kept at 500 °C for half an hour. An iodine-based liquid electrolyte (100mM lithium iodide (LiI), 100 mM iodine (I_2), 500 mM 4-tert-butylpyridine (TBP), 600mM tetrabutylammonium iodide (TBAI) in acetonitrile solution) was utilized while assembling the two electrodes into a sandwich-type cell.

2.5. Computational detail

Density functional theory (DFT) calculations were employed using the hybrid B3LYP functional and 6-31+ G (d,p) basis set to compare the electronic properties and geometries of Car-Cy, Car-Mal and Car-Amin [45]. All structural optimization and energy calculations were performed using the Gaussian 09 program package [46]. The vibrational frequency calculations were performed to confirm that all optimized geometries were local minima. The time-dependent DFT (TD-DFT) was carried out to find the lowest vertical excitation energies of the synthesized compounds. The electronic structure and TD-DFT calculations were performed in DMF solution, using the conductor-like polarizable continuum *model* (***CPCM***) to characterize the UV-Vis spectrum and frontier molecular orbital energies, at B3LYP/6-31+G (d,p) levels of theory [47].

3 Results and discussion

3.1 The optical characteristics

The UV–visible spectra of Car-Cy, Car-Amin, and Car-Mal in DMF solution (10^{-5} M) have been depicted in Figure 2. The recorded spectra for Car-Cy and Car-Mal dyes display two distinct peaks: the first peak at 296 - 309 nm is related to the π–π^* electron transition, whereas the second peak at 392–397 nm is attributed to the intramolecular charge transfer (ICT) from carbazole to the acceptor group [48]. However, the dye Car-Amin exhibits three distinct bands: two bands in the UV region (~298 nm and ~336 nm) corresponding to the π-π^* electron transition. Whereas the third peak in the visible region (426 nm) is possibly attributed to the intramolecular charge transfer (ICT) from carbazole to the acceptor group [49]. The coefficient of molar extinction (ε) at the maximum absorption (λ_{max}) of ICT for Car-Cy, Car-Amin and Car-Mal were determined to be 52,457, 69,265 and 45,260 M^{-1} cm^{-1}, respectively. These data cleary demonstrate the excellent light harvesting capacity of the synthesized dyes (Table 1).

The ICT absorption peak of a dye on the TiO_2 film exhibits a red or blue shift compared with that in solution. This is because of the interaction between the dye and TiO_2 which leads to the accumulation of dye on the surface of titanium dioxide, resulting in a J- and H-aggregation for a red and blue shift, respectively. As shown in Table 1 and Figure 3, the absorption spectrum of dyes on the TiO_2 films were expanded, and the maximum absorption peaks for Car-Cy, Car-Amin, and Car-Mal were observed at 352, 424, 364 nm, demonstrating a blue shift of 45, 2, and 28 nm in comparison with those in DMF solution, respectively. H-aggregation or deprotonation of the dyes on the titanium dioxide surface can be good reasons for this blue shift [50]. Interestingly, the dye Car-Amin exhibits a much less blue shift with no remarkable differences as compared with that in DMF solution, which can imply that there is less aggregation of this dye on the TiO_2 surface [51].

This phenomenon may indicate that the dye Car-Amin can generate the highest open- circuit photo voltage (V_{oc}) value among other two dyes, which is in favor of a better photovoltaic performance. The broader absorption of dye Car-Amin on the TiO_2 film is beneficial to improve the light-harvesting capability, resulting in the higher photocurrent density and IPCE value [52].

Since dyes tend to accumulate at the solid-liquid interface, the blue shift often occurs for the organic dyes [53]. Furthermore, the adsorption of dyes on TiO_2 film makes the carboxylic acid group deprotonated, thus the capability of the TiO_2–carboxylate group as the acceptor will be less than the carboxylic acid itself [54]. So, all of the discussed issues can be effective in the observed blue shift. The interaction between titanium dioxide film and the dye broadens the absorption spectra, which is absolutely favorable in the production of light harvesting devices since it can possibly improve the photocurrent [55].

Fluorescence emission spectra of Car-Cy, Car-Amin, and Car-Mal were recorded in DMF solution (10^{-5} M) upon their excitation at their absorption wavelengths (λ_{abs}). Figure 4 exhibits the emission spectra of dyes and their outcomes are summarized in Table 1. As can be seen, the dyes show emission maxima in wavelength range of 524–560 nm which is in the same trend as observed in the absorbance spectra. Furthermore, Stokes shift values of dyes were calculated from their normalized UV-Vis absorption and fluorescence emission spectral data (Table 1)[56]. The Stokes shift values for the sensitizers were estimated to be in the range of 132-134 nm, exhibiting the efficient electron shift from donor unit (carbazole) to the acceptor / anchoring groups. In addition, optical band gaps (E_{0-0}) of the synthesized dyes were determined from the intersection of absorption and emission spectra and their calculated values are summarized in Table 1.

Table 1. The electrochemical and optical characteristics of the examined dyes.

Dyes	Car-Cy	Car-Amin	Car- Mal
HOMO/LUMO[a](ev)	-5.98/-3.40	-5.68/-2.98	-5.72/-2.94
Band gap[a]	2.57	2.70	2.78
λ_{abs} [b] (nm)/(ε M^{-1} cm^{-1})	397/52,457	426/69,265	392/45,260
λ_{em} (nm)	530	560	524
Stokes shift (nm)	133	134	132
λ_{max}[c] (nm)	352	424	364
HOMO[d] (eV)	-5.95	-5.99	-5.6
E_{0-0} [e](eV)	2.68	2.61	2.75
LUMO[f] (eV)	-3.27	-3.38	-2.85

[a]DFT computed energy values; [b]Absorption wavelengths of charge-transfer transition were evaluated in DMF; [c]Maximum absorption wavelength on TiO_2 films; [d]HOMO values were obtained using CV in DMF with 0.1 M tetrabutylammonium tetrafluoroborate; [e]E_{0-0} = 1240/λ intersection; [f]LUMO values were computed using HOMO+E_{0-0}.

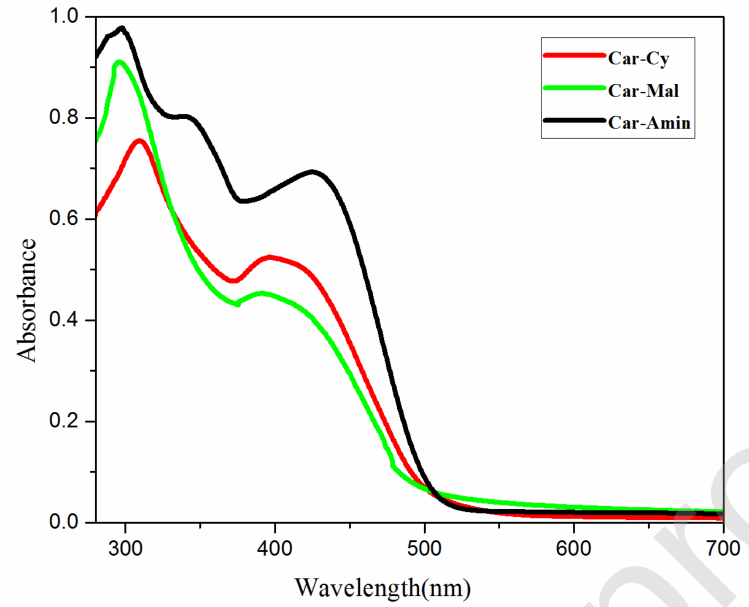

Figure 2. The recorded absorption spectra for the examined dyes in the DMF solution.

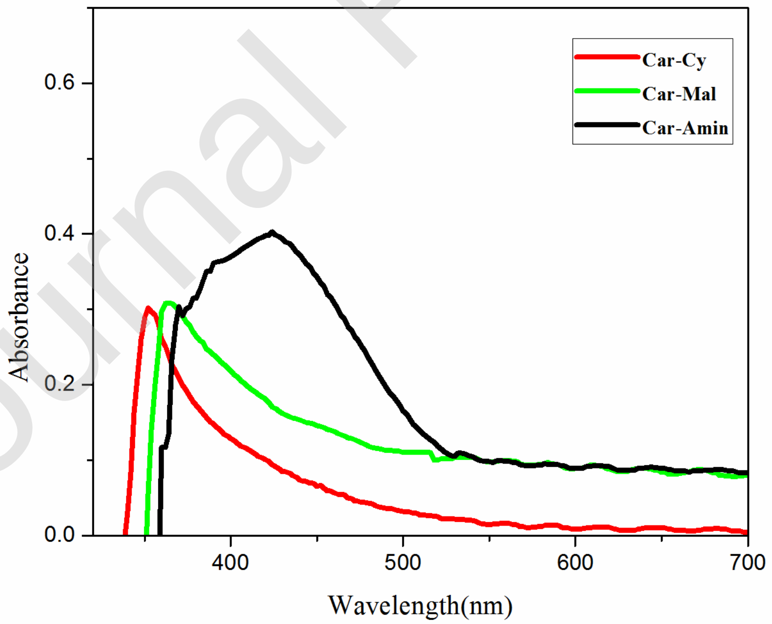

Figure 3. The recorded absorption spectra for the examined dyes absorbed on TiO_2 films.

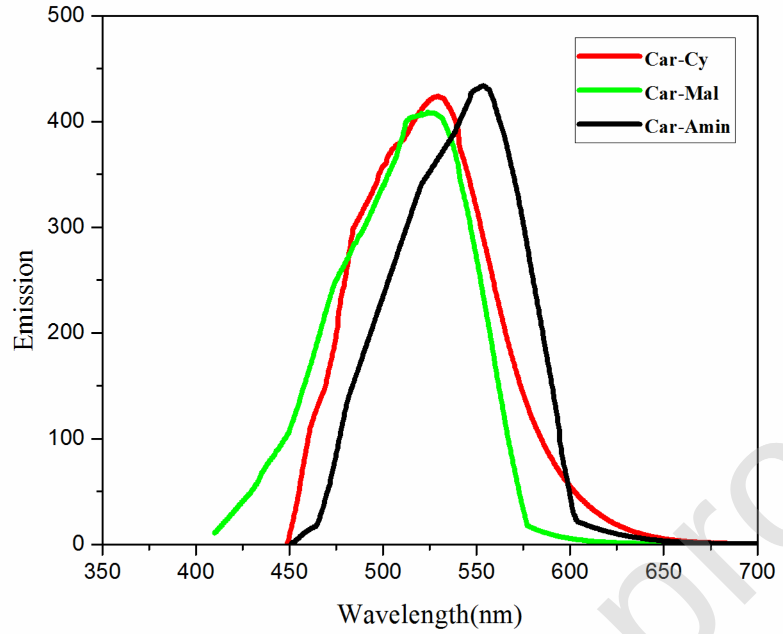

Figure 4. The recorded fluorescence emission spectra for the examined dyes in the DMF solution.

3.2 Electrochemical properties

The highest occupied molecular orbital (HOMO) and lowest unoccupied molecular orbital (LUMO) values of the prepared sensitizers were assessed by carrying out CV experiments. The obtained values can evaluate the thermodynamic possibility of electron injection from the LUMO of the dye molecule into the conduction band edge of the titanium dioxide semiconductor, and they can assess the capability of the redox electrolyte for regenerating the dye through refilling the generated hole in the HOMO. Figure 5 presents the results of the CV experiment. Also, the data and a graphical presentation of the measured HOMO and LUMO levels have been presented in Table 1, and Figure 6, respectively.

The first oxidation potentials (E_{ox}) of Car-Cy, Car-Amin, and Car-Mal were found to be 1.25, 1.29, and 0.9 V (vs. NHE), respectively. HOMO levels of dyes were determined from their first oxidation potentials (E_{ox}) using equation (1) [56].

$$\mathrm{HOMO} = -[E_{ox} + 4.7\ \mathrm{eV}] \qquad (1)$$

. Since these values for all of the examined dyes are more positive in comparison with the redox potential of the I_3^-/I^- electrolyte system (-5.2 eV), it can be concluded that there is sufficient power for the regeneration of the dyes. Moreover, the energy difference between the excited and ground states of the dyes ($E_{0–0}$) was calculated with $E_{0–0} = 1240/\lambda_{int}$, in which, λ_{int} is the intersection of the emission and absorption spectra. The λ_{int} values for the Car-Cy, Car-Amin, and Car-Mal were found to be 461, 474 and 450 nm, respectively. The values of $E_{0–0}$ have been presented in Table 1. The LUMO levels were determined using equation (2).

$$\mathrm{LUMO} = \mathrm{HOMO} + E_{0–0} \qquad (2)$$

These values for the Car-Cy, Car-Amin, and Car-Mal were found to be -3.27, -3.38 and -2.85 eV, respectively, and since they are more negative than the conduction band of titanium dioxide (− 4.2 eV), the electron injection from the dyes into TiO_2 is possible. Consequently, it can be assumed that the synthesized dyes in this study are potential sensitizers in DSSCs.

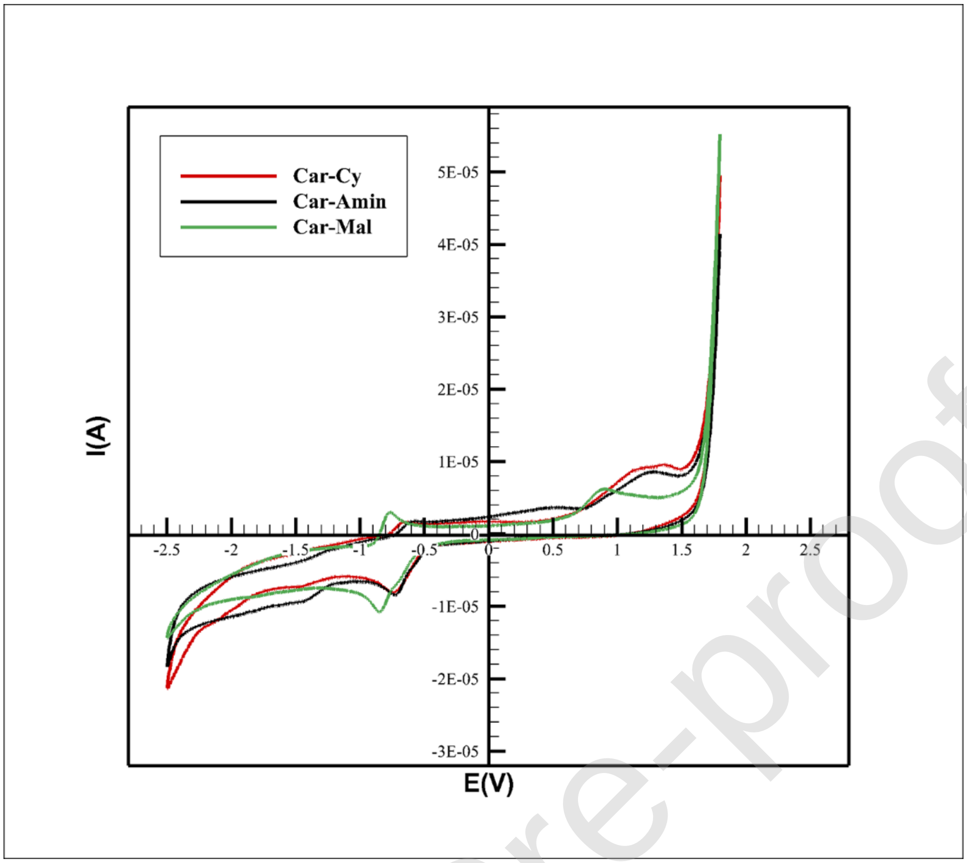

Figure 5. The recorded CV results for the examined dyes in the DMF solutions.

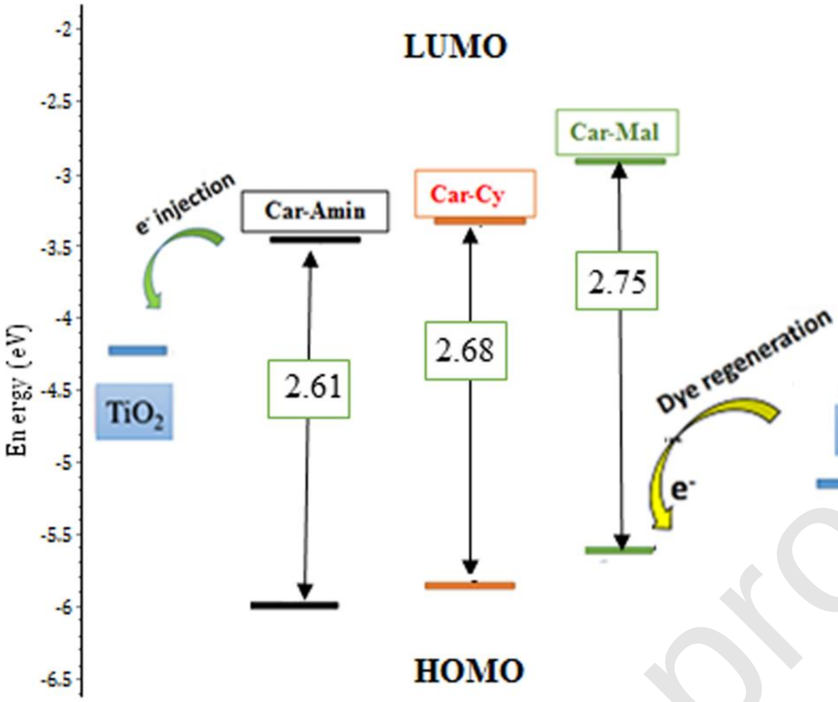

Figure 6. The schematic of the energy levels in the examined dyes based on absorption and electrochemical characteristics.

3.3 Theoretical investigations

The DFT computations are known as one of the important computational investigations and are broadly applied in the DSSC systems to get a better look at the electronic properties and molecular structure of the sensitizers [57, 58]. Figure 7 illustrates the optimized molecular structures as well as the distribution of the electron density in their related frontier molecular orbital (FMO) energy levels.

The results of natural bond orbital (NBO) studies indicate that the HOMO electron density are frequently delocalized on donor (carbazole ring) and π-linker (vinyl thiophene) segments, whereas, the LUMO electrons are obviously transferred from carbazole to the acceptors (cyanoacetic acid, 4-aminobenzoic acid, and malonic acid). The extent of this transformation depends on the nature of electron-withdrawing groups of the acceptor [56]. In addition, it is worth to mention that the electron cloud of LUMO energy level in the examined dyes was only shifted toward the acceptor/anchoring unit connected to the vinyl thiophene π-spacer and not the anchoring group connected to vinylene unit [59]. This observation can be due to the higher abundance of electrons in the π-conjugation section, which results in more interactions between the acceptor and donor [60]. The theoretical data show that the HOMO levels obtained for dyes Car-Cy (-5.98 eV), Car-Mal (-5.72 eV) and Car-Amin (-5.68 eV) are sufficiently lower than the electrode potential of redox couple (-5.2 eV) facilitating the regeneration process. Likewise, obtained LUMO levels of Car-Cy (-3.40 eV), Car-Mal (-2.94 eV) and Car-Amin (-2.98 eV) clearly show that, electron injection is also facilitated as the values are higher than the CB of TiO_2 (-4.2 eV). Therefore, from theoretical point of view, these dyes are also useable in DSSCs. The theoretical HOMO and LUMO levels are close to the experimental data obtained from cyclic voltammograms (Table 1).

Furthermore, TD-DFT calculations were performed to elucidate the electronic transitions and also to interpret of UV-Vis spectrum of all three compound in solution. The maximum absorption wavelengths, oscillator strength (*f*) and corresponding transition assignment are listed in Table 2, and the absorption spectra are shown in Figure 8. The data show that the lowest energy transition of the dyes corresponds to HOMO→LUMO excitation. Therefore, the bands seen in the visible region of the experimental absorption spectra include the HOMO → LUMO transitions. The red shift of λ_{max} from theory to experiment is associated to the self-interaction error in TD-DFT arising through the electron transfer in the extended charge-transfer state (Figure 8) [61]. The other transitions involve HOMO-1 → LUMO, HOMO → LUMO +1 and HOMO → LUMO +2 corresponding to the π-π* transitions. In addition, the *f* calculated for the aforementioned transition is 1.56 for Car-Cy, 1.45 for Car-Mal and 1.78 for Car-Amin, respectively, which is consistent with the trend of molar extinction coefficients (Table 2). Therefore, from these observations, it can be mentioned that the theoretical absorption spectra are in accordance with the experimentally ones. However, Car-Cy dye shows slightly more red-shift comparing to the other dyes, which could be related to the effect of functional and basis set on the energy levels [62].

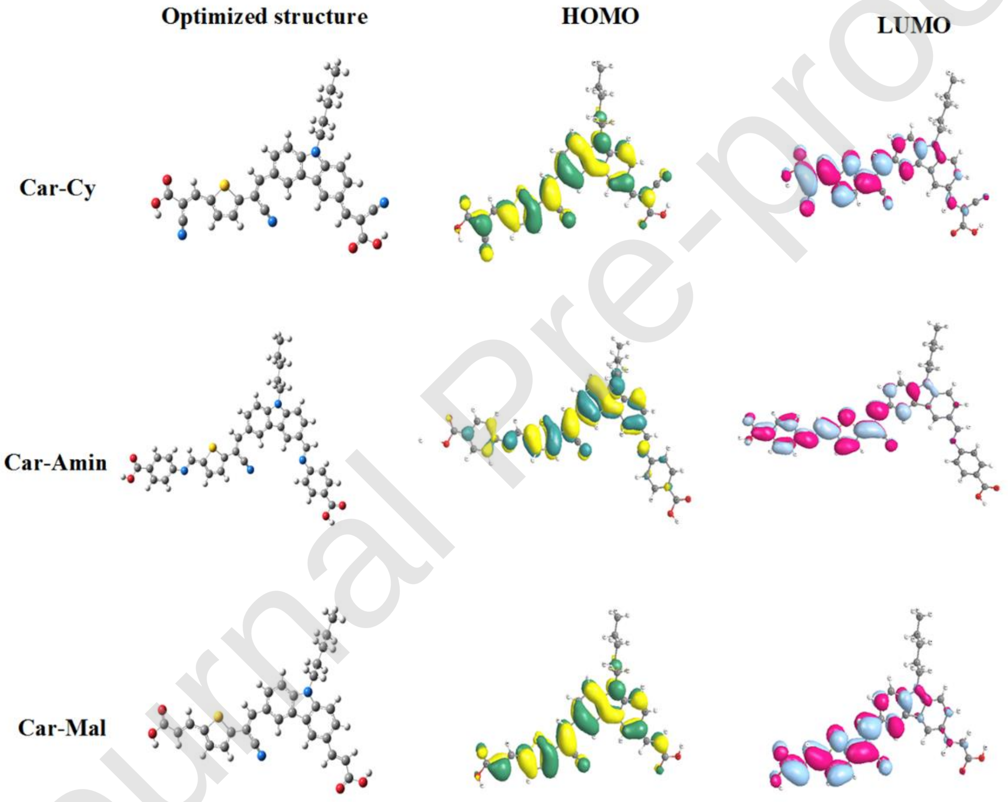

Figure 7. The FMOs of the HOMO and LUMO from the DFT computations.

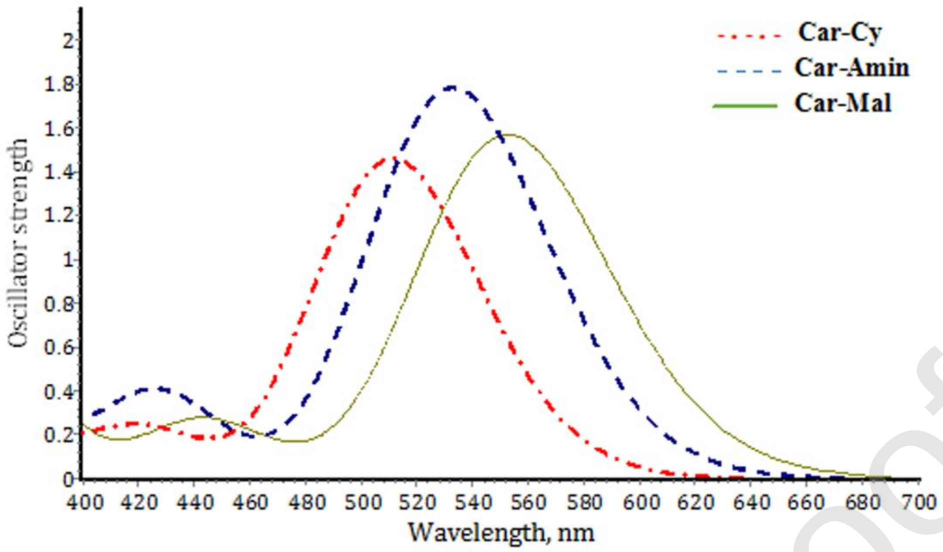

Figure 8. The TD-DFT absorbance spectra of dyes calculated with B3LYP/6-31+G (d, p) level.

Table 2. Maximum absorption wavelengths, orbital energies, oscillator strength (*f*) and assignment of synthesized dyes in DMF solution optimized at B3LYP/61+G (d, p) level.

Dyes	λ_{max} *(Experimental)*	λ_{max} *(B3LYP)*	*Composition (%)*	*E (eV)*	*f*
Car-Cy	397 309	552.6 448.1 438.5	H→L (70.0) H-1→L (63.0) H→L+2 (63.0)	2.24 2.76 2.83	1.56 0.15 0.13
Car-Amin	426 298,336	533.1 431.0 419.3	H→L (70.0) H-1→L (70.0) H→L+1 (69.0)	2.32 2.87 2.95	1.78 0.25 0.17
Car-Mal	392 296	511.3 423.7	H→L (70.0) H-1→L (69.0)	2.42 2.92	1.45 0.21

3.4 Photovoltaic performance

To establish the applicability of the prepared dyes as sensitizers, DSSC devices were constructed using the synthesized dyes and their performance was studied. The photovoltaic parameters including PCE, fill factor (FF), V_{OC} and short-circuit photocurrent density (J_{SC}) were measured for the constructed devices and the obtained results have been summarized in Table 3. Figure 9 presents the Current-Voltage (J–V) curves for sensitizer-based DSSCs.

As is clear in Table 3, the maximum PCE, J_{SC}, and V_{OC}, with the values of 2.27%, 5.95 mA/cm^2, and 0.54 V, respectively, were observed for the Car-Amin dye. The J_{SC} value of Car-Amin is also bigger than that in the other dyes which could be related to its greater molar extinction coefficient (Table 1) [63]. Reports have also shown that a higher value of J_{sc} can be effective in obtaining greater PCE percentages [43]. According to the results, the photovoltaic performance of the examined dyes follows this order: Car-Amin > Car-Cy > Car-Mal. The higher performance of the Car-Amin dye could be due to the good electron-withdrawing ability from carbazole donor followed by good efficiency of 4-aminobenzoic acid anchoring group in injecting electrons into the conduction band edge of titanium dioxide. These observations are well compatible with the previous reports in similar studies [64]. The data of Figure 9 further confirms the influence of acceptor/anchoring groups on the DSSC device performance. As can be observed, when malonic acid was used as the anchoring group, the corresponding dye that is, Car-Mal presented lower J_{sc} and PCE (4.99 mA cm^{-2} and 1.69%, respectively) in comparison with the other investigated dyes. The results of this research revealed that the efficiency of anchoring/acceptor groups in constructed devices follows this order: 4-aminobenzoic acid > cyanoacetic acid > malonic acid. Therefore, among the used acceptors, 4-aminobenzoic acid showed to be a better electron acceptor that can be attached to TiO_2 more efficiently. Also, we have compared the solar cell efficiency of the synthesized dyes in this study with a few of similar carbazole dyes reported in the literatures in Table S1 (supporting Information). It can be seen that, although we have not used any auxiliary components in the solar cells, the efficiency of the studied dyes is relatively comparative with those reported previously.

The IPCE curves of the synthesized dyes have been illustrated in Figure 10. The IPCE spectra confirm that the pattern of the measured Jsc values for the examined dyes (Car-Amin > Car-Cy > Car-Mal) is in agreement with the observed trend for their absorption characteristics. By comparing the IPCE curves with the absorption spectra of the attached dyes to titanium dioxide, a red shift can be seen in the IPCE spectra, which might be due to side interactions in the dyes layer [43]. The results clearly show that the IPCE spectra of Car-Amin display a broad band between 400 and 610 nm with a maximum percentage of 62.2% at 465 nm which might contribute to higher photocurrent density and J_{sc} of Car-Amin dye, that is further confirmed by the amounts of dye adsorbed on the TiO_2 film as measured using the UV-Vis absorptions (Table 3). Generally, the existence of a broad band in the IPCE spectra is favorable for obtaining a larger photocurrent. This explains the observed difference in PCE percentages of the examined dyes [65]. The better IPCE response of Car-Amin can be demonstrated by the higher J_{SC} value for this dye (5.95 mA.cm^{-2}) in comparison with those of Car-Cy (5.66 mA.cm^{-2}), and Car-Mal (4.99 mA.cm^{-2}), which indicates the effectiveness of A-π-D-π-A-π-A architecture on improving the DSSC efficiency.

All of the results suggest that the introduction of 4-aminobenzoic acid as an electron acceptor leads to enhancement of the absorption characteristics and improvement of the J_{sc} values. Thus, the usage of 4-aminobenzoic acid as the electron acceptor in the Car-Amin structure can be the important reason for obtaining the better photovoltaic performance than the other examined dyes.

Table 3. DSSC performance data of the dyes.

Sample	*J_{sc} (mA.cm^{-2})*	*V_{oc} (V)*	*FF (%)*	*PCE (%)*	*[a]Dye loading(mol.cm^{-2})*
Car-Cy	5.66	0.52	72	2.14	2.37×10^{-7}
Car-Mal	4.99	0.48	71	1.69	1.92×10^{-7}
Car-Amin	5.95	0.54	71	2.27	3.93×10^{-7}

[a]Dye adsorption on TiO_2 was measured from the subtraction of the UV–Vis absorption of dye solution before and after dipping of the TiO_2 film in dye solution

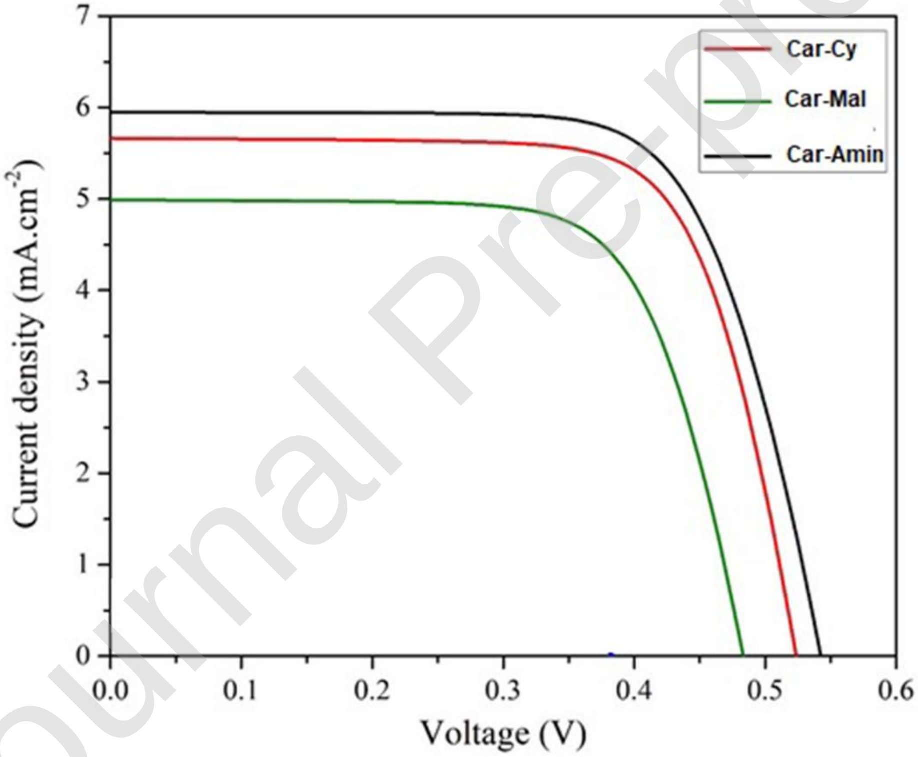

Figure 9. The J–V curves for the DSSCs with the examined dyes.

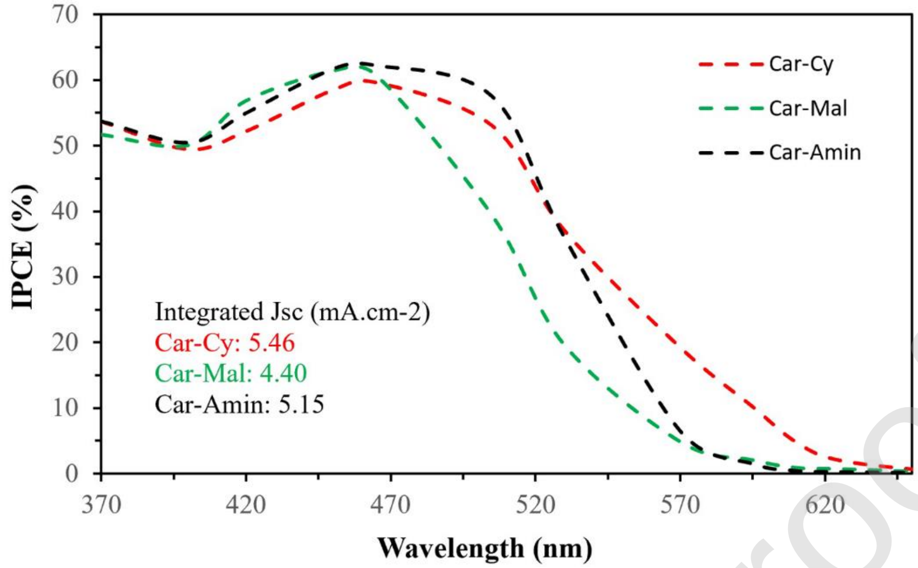

Figure 10. The IPCE spectra for the examined dyes.

3.5 The EIS Analysis

The EIS is a widely employed technique for recognizing the electron lifetime and the electrochemical behavior of the constructed DSSCs [66, 67]. The Nyquist plots of the constructed devices using the synthesized sensitizers have been shown in Figure 11. It is obvious that all the dyes exhibited two semicircles related to recombination resistance at the Pt/electrolyte interface (first semicircle) and Titanium dioxide/dye/electrolyte interface (second semicircle). Modifying the TiO_2 surface with different dyes could change the electron transfer between electrolyte and dye or dye and TiO_2, hence a significant difference in the radius of the second semicircles appears in the EIS curves. The radius of the second semicircle was measured from Figure 11, then it was used to calculate the charge recombination resistance (R_{ct}). The R_{ct} values were determined to be 6.50 Ω for Car-Cy, 9.70 Ω for Car-Amin and 11.52 Ω for Car-Mal. The higher R_{ct} value for the Car-Mal results in a slow charge recombination between the oxidized species and TiO_2.

Another critical parameter for constructed devices is the electron lifetime (τ), which can be determined using the available data in the EIS curves. Chemical capacitances (C_μ) and R_{ct} were used in the formula: $\tau = C_\mu \times R_{ct}$ to calculate the electron lifetime [43]. It should be noted that the C_μ values were found to be 6.75 μF/Cm^2 for Car-Cy, 11.76 μF/Cm^2 for Car-Amin and 1.92 μF/Cm^2 for Car-Mal. Generally, a longer electron lifetime in the conduction band of titanium dioxide is favorable, because it suppresses the back-reaction between the injected electrons into titanium dioxide and the electrolyte, and also, results in enhancements in V_{OC} values [68]. Based on the results, the electron lifetime values in the conduction band edge of titanium dioxide for the manufactured devices with the examined dyes followed this order: Car-Amin (11.41 ms) >Car-Cy (4.39 ms) >Car-Mal (2.22 ms). These observations indicate that the Car-Amin sensitizer containing 4-aminobenzoic acid as the acceptor system can efficiently reduce the undesired charge recombination. In addition, the estimated lifetime of the dyes was well-compatible with the experimental V_{OC} values obtained from the devices (Table 3). The V_{oc} values follow this order: Car-Amin > Car-Cy > Car-Mal.

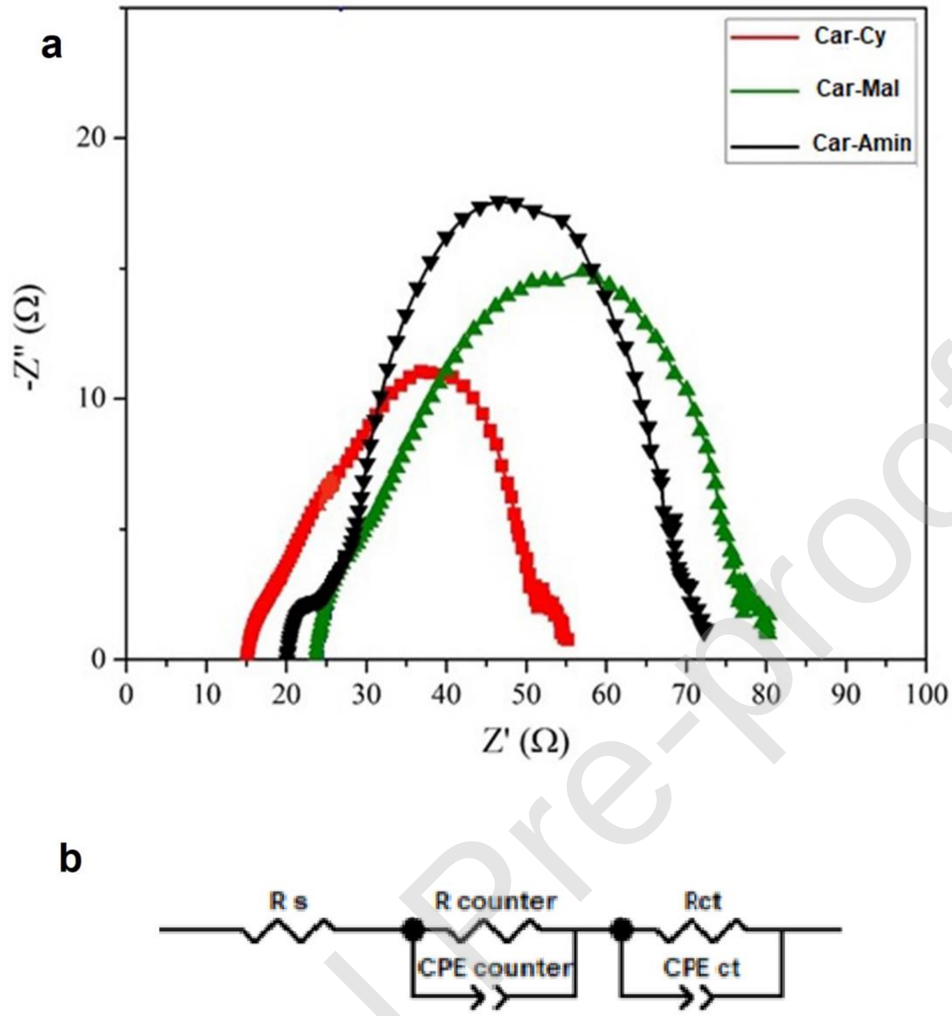

Figure 11. The EIS spectra of the prepared DSSCs, (**a),** Nyquist plots and (**b),** equivalent circuit.

4 Conclusion

In this study, three novel carbazole-based dyes, including Car-Cy, Car-Amin, and Car-Mal, with the A-π-D-π-A-π-A architecture were designed, synthesized and fully-analyzed by different methods. The synthesized di-anchoring unsymmetrical organic dyes were efficiently applied as sensitizers in DSSCs and exhibited good electrochemical and optical characteristics as well as favorable photovoltaic performances in solar cells.

The constructed device using Car-Amin dye with 4-aminobenzoic acid as an acceptor unit exhibited a PCE of 2.27%, IPCE response of 62.2%, J_{SC} value of 5.95 $mA.cm^{-2}$ and V_{OC} of 0.54 V, which were better than the corresponding values for the other tested dyes. Furthermore, the EIS investigations indicated that among the examined dyes, Car-Amin has a higher ability to control the unwanted charge recombination in the DSSC and consequently can extend the electron lifetime. The larger electron lifetime in the conduction band edge of titanium dioxide in the constructed DSSC device with Car-Amin results in a higher V_{OC} value with this dye. The findings of this study revealed that selecting 4-aminobenzoic acid as an acceptor/anchoring group can significantly affect photovoltaic performance. Also, the results showed that the structural modification of organic sensitizers is a useful technique for fabricating more enhanced devices.

Author statement

I sincerely appreciate for giving us an opportunity to revise our manuscript. All the editorial and reviewer's comments were precisely examined and the relevant responses were provided for each comment. The conducted modifications of the manuscript were highlighted with a yellow background and explained at the end of this mail. However, if there is anything else should be done, please let me know.

Once again I would appreciate your kind consideration of the manuscript and remaining hearing from you.

Declaration of interests

The authors declare that they have no known competing financial interests or personal relationships that could have appeared to influence the work reported in this paper.

Acknowledgments

The authors of this research appreciate the University of Mazandaran and the Iran National Science Foundation (INSF) for financially supporting this work.

References

[1] B. O'regan, M.Grätzel, A low-cost, high-efficiency solar cell based on dye-sensitized colloidal TiO_2 films, Nature 353 (1991) 737-740. https://doi.org/10.1038/353737a0.

[2] M. Grätzel, Solar energy conversion by dye-sensitized photovoltaic cells, Inorg. Chem. 44 (2005) 6841-6851. https://doi.org/10.1021/ic0508371.

[3] H. Cheema, A. Islam, R. Younts, B. Gautam, I. Bedja, R.K. Gupta, L. Han, K. Gundogdu, A. El-Shafei, More stable and more efficient alternatives of Z-907: carbazole-based amphiphilic

Ru (II) sensitizers for dye-sensitized solar cells, Phys. Chem. Chem. Phys. 16 (2014) 27078-27087. https://doi.org/10.1039/C4CP04120H.

[4] A. Morandeira, I. López-Duarte, B. O'Regan, M. V. Martínez-Díaz, A. Forneli, E. Palomares, T. Torres, J. R. Durrant, Ru (II)-phthalocyanine sensitized solar cells: the influence of co-adsorbents upon interfacial electron transfer kinetics, J. Mater. Chem. 19 (2009) 5016-5026. https://doi.org/10.1039/B904179F.

[5] M. K. Nazeeruddin, A. Kay, I. Rodicio, R. Humphry-Baker, E. Müller, P. Liska, N. Vlachopoulos, M. Grätzel, Conversion of light to electricity by cis-X2bis (2, 2'-bipyridyl-4, 4'-dicarboxylate) ruthenium (II) charge-transfer sensitizers (X= Cl^-, Br^-, I^-, CN^-, and SCN^-) on nanocrystalline titanium dioxide electrodes, J. Am. Chem. Soc. 115 (1993) 6382-6390. https://doi.org/10.1021/ja00067a063.

[6] M. K. Nazeeruddin, S. M. Zakeeruddin, R. Humphry-Baker, M. Jirousek, P. Liska, N. Vlachopoulos, V. Shklover, C. H. Fischer, M. Grätzel, Acid− base equilibria of (2, 2 ‘-Bipyridyl-4, 4 ‘-dicarboxylic acid) ruthenium (II) complexes and the effect of protonation on charge-transfer sensitization of nanocrystalline titania, Inorg. Chem. 38 (1999) 6298-6305. https://doi.org/10.1021/ic990916a.

[7] Y. Tang, Y. Wang, X. Li, H. Ågren, W. H. Zhu, Y. Xie, Porphyrins containing a triphenylamine donor and up to eight alkoxy chains for dye-sensitized solar cells: a high efficiency of 10.9%, ACS. Appl. Mater. Interfaces. 7 (2015) 27976-27985. https://doi.org/10.1021/acsami.5b10624.

[8] H.-Y Wang, F. Liu, L. H. Xie, C. Tang, B. Peng, W. Huang, W. Wei, Topological arrangement of fluorenyl-substituted carbazole triads and starbursts: synthesis and optoelectronic properties, J. Phys. Chem. C. 115 (2011) 6961-6967. https://doi.org/10.1021/jp200433e.

[9] J.-H Yum, E. Baranoff, S. Wenger, M. K. Nazeeruddin, M.Grätzel, Panchromatic engineering for dye-sensitized solar cells, Energy Environ. Sci. 4 (2011) 842-857. https://doi.org/10.1039/C0EE00536C.

[10] D.D.Babu, H. Cheema, D. Elsherbiny, A. El-Shafei, A. V. Adhikari, Molecular engineering and theoretical investigation of novel metal-free organic chromophores for dye-sensitized solar cells, Electrochim. Acta. 176 (2015) 868-879. https://doi.org/10.1016/j.electacta.2015.07.079.

[11] H. Choi, C. Baik, S. Kim, M. S. Kang, X. Xu, H. S. Kang, S. O. Kang, J. Ko, M. K. Nazeeruddin, M. Grätzel, Molecular engineering of hybrid sensitizers incorporating an organic antenna into ruthenium complex and their application in solar cells, New J. Chem. 32 (2008) 2233-2237. https://doi.org/10.1039/B810332A.

[12] G. Li, K. J. Jiang, P. Bao, Y. F. Li, S. L. Li, L. M. Yang, Molecular design of triarylamine-based organic dyes for efficient dye-sensitized solar cells, New J. Chem. 33 (2009) 868-876. https://doi.org/10.1039/B815649B.

[13] A. Mishra, M. K. Fischer, P. Bäuerle, Metal-free organic dyes for dye-sensitized solar cells: from structure: property relationships to design rules, Angew. Chem. Int. Ed. 48 (2009) 2474-2499. https://doi.org/10.1002/anie.200804709.

[14] M. U. Khan, M. Ibrahim, M. Khalid, S. Jamil, A. A. Al-Saadi, M. R. S. A. Janjua, Quantum chemical designing of indolo [3, 2, 1-jk] carbazole-based dyes for highly efficient nonlinear optical properties, Chem. Phys. Lett. 719 (2019) 59-66. https://doi.org/10.1016/j.cplett.2019.01.043.

[15] C. Luo, W. Bi, S. Deng, J. Zhang, S. Chen, B. Li, Q.Liu, H.Peng, J.Chu, Indolo [3, 2, 1-jk] carbazole derivatives-sensitized solar cells: effect of π-bridges on the performance of cells, J. Phys. Chem. C, 118(2014) 14211-14217. https://doi.org/10.1021/jp503455m.

[16] M. A. Reddy, B. Vinayak, T. Suresh, S. Niveditha, K. Bhanuprakash, S. P. Singh, A. Islam, , L. Han, M. Chandrasekharam, Highly conjugated electron rich thiophene antennas on phenothiazine and phenoxazine-based sensitizers for dye sensitized solar cells, Synth. Met. 195 (2014) 208-216. https://doi.org/10.1016/j.synthmet.2014.06.009.

[17] X. Zhang, Y. Xu, F. Giordano, M. Schreier, N. Pellet, Y. Hu, C. Yi, N. Robertson, J. Hua, S. M. Zakeeruddin, H. Tian, Molecular engineering of potent sensitizers for very efficient light harvesting in thin-film solid-state dye-sensitized solar cells, J. Am. Chem. Soc. 138 (2016) 10742-10745. https://doi.org/10.1021/jacs.6b05281.

[18] L. Han, H. Wu, Y. Cui, X. Zu, Q. Ye, J. Gao, Synthesis and density functional theory study of novel coumarin-type dyes for dye sensitized solar cells, J. Photochem. Photobiol. A: Chem. 290 (2014) 54-62. https://doi.org/10.1016/j.jphotochem.2014.06.001.

[19] K. Funabiki, H. Mase, Y. Saito, A. Otsuka, A. Hibino, N. Tanaka, H. Miura, Y. Himori, T. Yoshida, Y. Kubota, M. Matsui, Design of NIR-absorbing simple asymmetric squaraine dyes carrying indoline moieties for use in dye-sensitized solar cells with Pt-free electrodes, Org. Lett. 14 (2012) 1246-1249. https://doi.org/10.1021/ol300054a.

[20] S. Higashijima, Y. Inoue, H. Miura, Y. Kubota, K. Funabiki, T. Yoshida, M. Matsui, Organic dyes containing fluorene-substituted indoline core for zinc oxide dye-sensitized solar cell, RSC Adv. 2 (2012) 2721-2724. https://doi.org/ 10.1039/C2RA01358D.

[21] M. Marszalek, S. Nagane, A. Ichake, R. Humphry-Baker, V. Paul, S.M. Zakeeruddin, M. Grätzel, Tuning spectral properties of phenothiazine based donor–π–acceptor dyes for efficient dye-sensitized solar cells, J. Mater. Chem. 22 (2012) 889-894. https://doi.org/ 10.1039/C1JM14024H.

[22] R. Tarsang, V. Promarak, T. Sudyoadsuk, S. Namuangruk, S. Jungsuttiwong, Tuning the electron donating ability in the triphenylamine-based D-π-A architecture for highly efficient dye-sensitized solar cells, J. Photochem. Photobiol. A: Chem. 273 (2014) 8-16. https://doi.org/10.1016/j.jphotochem.2013.09.002.

[23] A.C. Onicha, K. Panthi, T.H. Kinstle, F.N. Castellano, Carbazole donor and carbazole or bithiophene bridged sensitizers for dye-sensitized solar cells, J. Photochem. Photobiol. A: Chem. 223 (2011) 57-64. https://doi.org/10.1016/j.jphotochem.2011.08.001.

[24] Y. Hao, X. Yang, J. Cong, A. Hagfeldt, L. Sun, Engineering of highly efficient tetrahydroquinoline sensitizers for dye-sensitized solar cells, Tetrahedron 68 (2012) 552-558. https://doi.org/10.1016/j.tet.2011.11.004.

[25] Y. Fu, J. Kim, A. Siva, W.S. Shin, S.J. Moon, T. Park, Parameters influencing the molecular weight of 3, 6-carbazole-based D-π-A-type copolymers, J. Polym. Sci. Part A: Polym. Chem. 49 (2011) 4368-4378. https://doi.org/10.1002/pola.24877.

[26] N. Blouin, A. Michaud, M. Leclerc, A low-bandgap poly (2, 7-carbazole) derivative for use in high-performance solar cells, Adv. Mater. 19 (2007) 2295-2300. https://doi.org/10.1002/adma.200602496.

[27] N. Koumura, Z. S. Wang, S. Mori, M. Miyashita, E. Suzuki, K. Hara, Alkyl-functionalized organic dyes for efficient molecular photovoltaics, J. Am. Chem. Soc. 128 (2006) 14256-14257. https://doi.org/10.1021/ja0645640.

[28] X. Liu, X. Ding, Y. Ren, Y. Yang, Y. Ding, X. Liu, A. Alsaedi, T. Hayat, J. Yao, S. Dai, A star-shaped carbazole-based hole-transporting material with triphenylamine side arms for perovskite solar cells. J. Mater. Chem. C, 6 (2018) 12912-12918. https://doi.org/10.1039/C8TC04191A.

[29] M. Li, S. Ma, M. Mateen, X. Liu, Y. Ding, J. Gao, Y. Yang, X. Zhang, Y. Wu, S. Dai, Facile donor (D)-π-D triphenylamine-based hole transporting materials with different π-linker for perovskite solar cells. Sol. Energy, 195(2020) 618-625. https://doi.org/10.1016/j.solener.2019.11.071.

[30] D. Joly, L. Pellejà, S. Narbey, F. Oswald, J. Chiron, J. N. Clifford, E. Palomares, R. Demadrille, A robust organic dye for dye sensitized solar cells based on iodine/iodide electrolytes combining high efficiency and outstanding stability, Sci. Rep. 4(2014) 4033. https://doi.org/10.1038/srep04033.

[31] H. C. Ting, C. H. Tsai, J. H. Chen, L. Y. Lin, S. H. Chou, K. T. Wong, T. W. Huang, C. C. Wu, A novel amine-free dianchoring organic dye for efficient dye-sensitized solar cells, Org. Lett. 14 (2012) 6338-6341. https://doi.org/10.1021/ol303121z.

[32] F. Ambrosio, N. Martsinovich, A. Troisi, Effect of the anchoring group on electron injection: theoretical study of phosphonated dyes for dye-sensitized solar cells, J. Phys. Chem. C 116 (2012) 2622-2629. https://doi.org/10.1021/jp209823t.

[33] R. Sirohi, D. H. Kim, S. C. Yu, S. H. Lee, Novel di-anchoring dye for DSSC by bridging of two mono anchoring dye molecules: a conformational approach to reduce aggregation, Dyes Pigments 92 (2012) 1132-1137. https://doi.org/10.1016/j.dyepig.2011.09.003.

[34] X. Sun, Y. Wang, X. Li, H. Ågren, W. Zhu, H. Tian, Y. Xie, Cosensitizers for simultaneous filling up of both absorption valleys of porphyrins: a novel approach for developing efficient panchromatic dye-sensitized solar cells, Chem. Commun. 50(2014) 15609-15612. https://doi.org/10.1039/C4CC07963A.

[35] T. Wei, X. Sun, X. Li, H. Agren, Y. Xie, Systematic investigations on the roles of the electron acceptor and neighboring ethynylene moiety in porphyrins for dye-sensitized solar cells, ACS Appl. Mater. Interfaces 7 (2015) 21956-21965. https://doi.org/10.1021/acsami.5b06610.

[36] A. Abbotto, N. Manfredi, C. Marinzi, F. De Angelis, E. Mosconi, J. H. Yum, Z. Xianxi, M. K. Nazeeruddin, M Grätzel, Di-branched di-anchoring organic dyes for dye-sensitized solar cells, Energy Environ. Sci. 2 (2009) 1094-1101. https://doi.org/10.1039/B910654E.

[37] X. Ren, S. Jiang, M. Cha, G. Zhou, Z. S. Wang, Thiophene-bridged double D-π-A dye for efficient dye-sensitized solar cell, Chem. Mater.24 (2012) 3493-3499. https://doi.org/10.1021/cm302250y.

[38] D. Cao, J. Peng, Y. Hong, X. Fang, L. Wang, H. Meier, Enhanced performance of the dye-sensitized solar cells with phenothiazine-based dyes containing double D− A branches, Org. Lett. 13 (2011) 1610-1613. https://doi.org/10.1021/ol2000167.

[39] W. I. Hung, Y. Y. Liao, C. Y. Hsu, H. H. Chou, T. H. Lee, W. S. Kao, J. T. Lin, High-performance dye-sensitized solar cells based on phenothiazine dyes containing double anchors and thiophene spacers, Chem. Asian. J. 9 (2014) 357-366. https://doi.org/10.1002/asia.201301228.

[40] Z. Iqbal, W. Q. Wu, H. Zhang, L. Han, X. Fang, L. Wang, D. B. Kuang, H. Meier, D. Cao, Influence of spatial arrangements of π-spacer and acceptor of phenothiazine based dyes on the performance of dye-sensitized solar cells, Org. Electron. 14 (2013) 2662-2672. https://doi.org/10.1016/j.orgel.2013.07.007.

[41] Q. Li, J. Shi, H. Li, S. Li, C. Zhong, F. Guo, M. Peng, J. Hua, J. Qin, Z. Li, Novel pyrrole-based dyes for dye-sensitized solar cells: from rod-shape to “H” type, J. Mater. Chem. 22 (2012) 6689-6696. https://doi.org/10.1039/C2JM30200D.

[42] H. Zhang, J. Fan, Z. Iqbal, D. B. Kuang, L. Wang, H. Meier, D. Cao, Novel dithieno [3, 2-b: 2′, 3′-d] pyrrole-based organic dyes with high molar extinction coefficient for dye-sensitized solar cells, Org. Electron. 14 (2013) 2071-2081. https://doi.org/10.1016/j.orgel.2013.04.046.

[43] S. M. J. Nabavi, B. Hosseinzadeh, M. Tajbakhsh, H Alinezhad, Three novel bis carbazole organic dyes for dye-sensitized solar cells, J. Mater. Sci: Mater. Electron. 29 (2018) 3270-3280. https://doi.org/10.1007/s10854-017-8262-y.

[44] Y. Wu, M. Marszalek, S. M. Zakeeruddin, Q. Zhang, H. Tian, M. Grätzel, W. Zhu, High-conversion-efficiency organic dye-sensitized solar cells: molecular engineering on D–A–π-A featured organic indoline dyes, Energy Environ. Sci. 5 (2012) 8261-8272. https://doi.org/10.1039/C2EE22108J.

[45] A. D. Becke, Becke’s three parameter hybrid method using the LYP correlation functional, J. Chem. Phys, 98 (1993) 5648-5652.

[46] M. J. Frisch, G.W. Trucks, H. B. Schlegel, G. E. Scuseria, M. A. Robb, J. R. Cheeseman, , G. Scalmani, V. Barone, B. Mennucci, G. A. Petersson, H. Nakatsuji, Gaussian 09 Revision A. 1 Gaussian Inc; 2009. *Wallingford CT*.

[47] J. Tomasi, B. Mennucci, R. Cammi, Quantum mechanical continuum solvation models, Chem. Rev. 105 (2005) 2999-3094. https://doi.org/10.1021/cr9904009.

[48] S. Roquet, A. Cravino, P. Leriche, O. Alévêque, P. Frere, J. Roncali, Triphenylamine-thienylenevinylene hybrid systems with internal charge transfer as donor materials for heterojunction solar cells, J. Am. Chem. Soc. 128 (2006) 3459-3466. https://doi.org/10.1021/ja058178e.

[49] S. Urnikaite, M. Daskeviciene, R. Send, H. Wonneberger, A. Sackus, I. Bruder, V. Getautis, Organic dyes containing a hydrazone moiety as auxiliary donor for solid-state DSSC applications, Dyes Pigments, 114 (2015) 175-183. https://doi.org/10.1016/j.dyepig.2014.11.012.

[50] P. Shen, X. Liu, S. Jiang, Y. Huang, L. Yi, B. Zhao, S. Tan, Effects of aromatic π-conjugated bridges on optical and photovoltaic properties of N, N-diphenylhydrazone-based metal-free organic dyes, Org. Electron. 12 (2011) 1992-2002. https://doi.org/10.1016/j.orgel.2011.08.010.

[51] H. Tian, X. Yang, R. Chen, R. Zhang, A. Hagfeldt, L. Sun, Effect of different dye baths and dye-structures on the performance of dye-sensitized solar cells based on triphenylamine dyes, J. Phys. Chem. C, 112(2008), 11023-11033. https://doi.org/10.1021/jp800953s.

[52] X. X. Dai, H. L. Feng, W. J. Chen, Y. Yang, L. B. Nie, L. Wang, D. B. Kuang, H. Meier, D. Cao, Synthesis and photovoltaic performance of asymmetric di-anchoring organic dyes, Dyes Pigments, 122 (2015) 13-21. https://doi.org/10.1016/j.dyepig.2015.06.004.

[53] W. Ying, F. Guo, J. Li, Q. Zhang, W. Wu, H. Tian, J. Hua, Series of new D-A-π-A organic broadly absorbing sensitizers containing isoindigo unit for highly efficient dye-sensitized solar cells, ACS Appl. Mater. Interfaces. 4 (2012) 4215-4224. https://doi.org/10.1021/am300925e.

[54] L. Y. Lin, C. H. Tsai, K. T. Wong, T. W. Huang, L. Hsieh, S. H. Liu, H. W. Lin, C. C. Wu, S. H. Chou, S. H. Chen, A. I. Tsai, Organic dyes containing coplanar diphenyl-substituted dithienosilole core for efficient dye-sensitized solar cells, J. Org. Chem. 75 (2010) 4778-4785. https://doi.org/10.1021/jo100762t.

[55] K. Hara, M. Kurashige, Y. Dan-oh, C. Kasada, A. Shinpo, S. Suga, K. Sayama, H. Arakawa, Design of new coumarin dyes having thiophene moieties for highly efficient organic-dye-sensitized solar cells, New J. Chem. 27 **(**2003) 783-785. https://doi.org/10.1039/B300694H.

[56] P. Naik, M. R. Elmorsy, R. Su, D. D. Babu, A. El-Shafei, A. V. Adhikari, New carbazole based metal-free organic dyes with D-π-A-π-A architecture for DSSCs: synthesis, theoretical and cell performance studies, Sol. Energy. 153 (2017) 600-610. https://doi.org/10.1016/j.solener.2017.05.088.

[57] B. Delley, An all-electron numerical method for solving the local density functional for polyatomic molecules, J. Chem. Phys. 92 (1990) 508-517. https://doi.org/10.1063/1.458452.

[58] S. Namuangruk, R. Fukuda, M. Ehara, J. Meeprasert, T. Khanasa, S. Morada, T. Kaewin, S. Jungsuttiwong, T. Sudyoadsuk, V. Promarak, D–D− π–A-type organic dyes for dye-sensitized solar cells with a potential for direct electron injection and a high extinction coefficient: synthesis, characterization, and theoretical investigation, J. Phys. Chem. C. 116 (2012) 25653-25663. https://doi.org/10.1021/jp304489t.

[59] P. Naik, R. Su, M. R. Elmorsy, A. El-Shafei, A. V. Adhikari, New di-anchoring A–π-D–π-A configured organic chromophores for DSSC application: sensitization and co-sensitization studies, Photochem. Photobiol. Sci. 17 (2018) 302-314. https://doi.org/10.1039/C7PP00351J.

[60] D. D. Babu, R. Su, P. Naik, A. El-Shafei, A. V. Adhikari, Synthesis and photovoltaic performance of a novel asymmetric dual-channel co-sensitizer for dye-sensitized solar cell beyond 10% efficiency, Dyes Pigments. 141 (2017) 112-120. https://doi.org/10.1016/j.dyepig.2017.02.010.

[61] Z. J. Chermahini, A. N. Chermahini, H. A. Dabbagh, B. Rezaei, N. Irannejad, The effects of second electron acceptor group on the performance of tetrazole-based nanocrystalline TiO_2 sensitizers in DSSCs. Spectrochimica Acta Part A: Molecular and Biomolecular Spectroscopy, 178 (2017) 79-85. https://doi.org/10.1016/j.saa.2017.01.061.

[62] D. D. Babu, D. Elsherbiny, H. Cheema, A. El-Shafei, A. V. Adhikari, Highly efficient panchromatic dye-sensitized solar cells: Synergistic interaction of ruthenium sensitizer with novel co-sensitizers carrying different acceptor units, Dyes Pigments, 132 (2016) 316-328. https://doi.org/10.1016/j.dyepig.2016.05.016.

[63] P. Naik, R. Su, M. R. Elmorsy, A. El-Shafei, A. V. Adhikari, Investigation of new carbazole based metal-free dyes as active photo-sensitizers/co-sensitizers for DSSCs, Dyes Pigments. 149 (2018) 177-187. https://doi.org/10.1016/j.dyepig.2017.09.068.

[64] P. Naik, R. Su, M. R. Elmorsy , D. D. Babu, A. El-Shafei, A V. Adhikari, Molecular design and theoretical investigation of new metal-free heteroaromatic dyes with D-π-A architecture as photosensitizers for DSSC application, J. Photochem. Photobiol. A: Chem. 345 (2017) 63-73. https://doi.org/10.1016/j.jphotochem.2017.05.033.

[65] P. Naik, A. Planchat, Y. Pellegrin, F. Odobel, A. V. Adhikari, Exploring the application of new carbazole based dyes as effective p-type photosensitizers in dye-sensitized solar cells, Sol. Energy. 157 (2017) 1064-1073. https://doi.org/10.1016/j.solener.2017.09.024.

[66] J. Bisquert, Chemical capacitance of nanostructured semiconductors: its origin and significance for nanocomposite solar cells, Phys. Chem. Chem. Phys. 5 (2003) 5360-5364. https://doi.org/10.1039/B310907K.

[67] F. Fabregat-Santiago, J. Bisquert, G. Garcia-Belmonte, G. Boschloo, A. Hagfeldt, Influence of electrolyte in transport and recombination in dye-sensitized solar cells studied by impedance spectroscopy, Sol. Energy Mater. Sol. Cells. 87 (2005) 117-131. https://doi.org/10.1016/j.solmat.2004.07.017.

[68] P. Naik, R. Su, M. R. Elmorsy, A. El-Shafei, A. V. Adhikari, New carbazole based dyes as effective co-sensitizers for DSSCs sensitized with ruthenium (II) complex (NCSU-10), J. Energy Chem. 27 (2018) 351-360. https://doi.org/10.1016/j.jechem.2017.12.013.